



Mechanistically-grounded pathways connect remotely sensed canopy structure to soil respiration



Laura J. Hickey ^{a,*}, Lucas E. Nave ^b, Knute J. Nadelhoffer ^c, Cameron Clay ^a, Alexandra I. Marini ^a, Christopher M. Gough ^a

^a Biology Department, Virginia Commonwealth University, Richmond, VA, USA

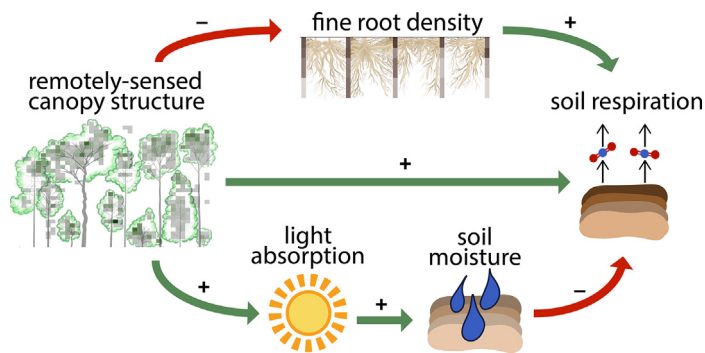
^b Biological Station and Department of Ecology and Evolutionary Biology, University of Michigan, Ann Arbor, MI, USA

^c Department of Ecology and Evolutionary Biology, University of Michigan, Ann Arbor, MI, USA

HIGHLIGHTS

- Lidar-derived canopy structure is related to soil respiration via multiple pathways.
- Canopy complexity is a stronger predictor of soil respiration than vegetation area.
- Complexity affects root density and soil moisture, factors tied to soil respiration.
- Canopy and root complexity are not spatially correlated at the stand scale.
- Spatial variation in soil respiration can be inferred from remotely-sensed structure.

GRAPHICAL ABSTRACT



ARTICLE INFO

Editor: Zhaozhong Feng

Keywords:

Lidar
Aboveground-belowground interactions
Fine root mass density
Soil microclimate
Structure-function
Rugosity

ABSTRACT

Variation in the soil-to-atmosphere C flux, or soil respiration (R_s), is influenced by a suite of biotic and abiotic factors, including soil temperature, soil moisture, and root biomass. However, whether light detection and ranging (lidar)-derived canopy structure is tied to soil respiration through its simultaneous influence over these drivers is not known. We assessed relationships between measures of above- and belowground vegetation density and complexity, and evaluated whether R_s is linked to remotely sensed canopy structure through pathways mediated by established biotic and abiotic mechanisms. Our results revealed that, at the stand-scale, canopy rugosity—a measure of complexity—and vegetation area index were coupled to soil respiration through their effects on light interception, soil microclimate, and fine root mass density, but this connection was stronger for complexity. Canopy and root complexity were not spatially coupled at the stand-scale, with canopy but not root complexity increasing through stand development. Our findings suggest that remotely sensed canopy complexity could be used to infer spatial variation in R_s , and that this relationship is grounded in known mechanistic pathways. The broad spatial inference of soil respiration via remotely sensed canopy complexity requires multi-site observations of canopy structure and R_s , which is possible given burgeoning open data from ecological networks and satellite remote sensing platforms.

* Corresponding author at: 1000 W. Cary St., Richmond, VA 23284, USA.

E-mail address: hickeylj@vcu.edu (L.J. Hickey).

1. Introduction

Forest canopy structural features are strongly tied to *aboveground* microclimate and production (Hardiman et al., 2011; Gough et al., 2019), but whether canopy structure also drives *belowground* carbon (C) cycling processes through its effects on soil microclimate and root structure is not known. Spatial variation in the soil-to-atmosphere C flux, or soil respiration (R_s) is influenced by a suite of canopy-influenced biotic and abiotic factors. For example, canopy structure affects light transmission (Ishii et al., 2004; Atkins et al., 2018a) and, in turn, soil microclimate (McCarthy and Brown, 2006; Forrester et al., 2012; Cai et al., 2021; Hardwick et al., 2015). In addition, canopy structure influence root allocation and biomass (Hopkins et al., 2013; Suchewaboripont et al., 2015) and, along with abiotic factors, constrain the spatio-temporal dynamics of soil respiration (Raich and Schlesinger, 1992; Wang et al., 2017). Moreover, canopy effects on root carbohydrate supply and exudation (Litton et al., 2007) couple canopy structure to soil respiration by affecting the metabolic activity of roots and microbes (Sun et al., 2017). The interacting biotic and abiotic pathways coupling canopy structure to soil respiration, however, have not been fully elucidated, limiting integrative understanding of these above and belowground structure-function interactions.

The remote sensing of forest canopy structure is an increasingly powerful tool for inferring ecosystem functioning. The few studies relating remotely sensed canopy structure to soil respiration have emphasized

linkages with aboveground vegetation area or canopy reflectance (Tanaka and Hashimoto, 2006; Katayama et al., 2009; Shi et al., 2016; D'Andrea et al., 2020; Cai et al., 2021) and have not considered canopy structural complexity, a potent predictor of aboveground C cycling processes. "Structural complexity" metrics generally summarize the heterogeneity of aboveground vegetation distribution (Hardiman et al., 2011), and can be derived from terrestrial light detection and ranging (lidar) measurements of horizontal and vertical vegetation distribution (Lim et al., 2003; Kane et al., 2013; Atkins et al., 2018b). Aboveground vegetation complexity metrics such as canopy rugosity (sensu Hardiman et al., 2011) are strongly correlated with stand-to-regional variation in forest primary production through their effects on light acquisition and light-use efficiency (Hickey et al., 2019; Gough et al., 2019). Similarly, conventional root structural metrics summarizing vertical biomass distributions and densities (Zhou and Shangguan, 2007; Greinwald et al., 2021) are correlated with spatial variation in soil respiration (Pregitzer et al., 1998). Spatial mirroring of above- and belowground vegetation structure, such as the coherence of root and canopy gaps, has been identified (Hardiman et al., 2017), but whether such relationships extend to canopy-root *complexity* measures is not known (Fig. 1). Therefore, while segments of the pathway connecting canopy structure and soil respiration provide a strong foundation of knowledge, a more integrative understanding of above-belowground interactions is required to enhance mechanistically-grounded inference of soil respiration using terrestrial remote sensing (Cavender-Bares et al., 2022).

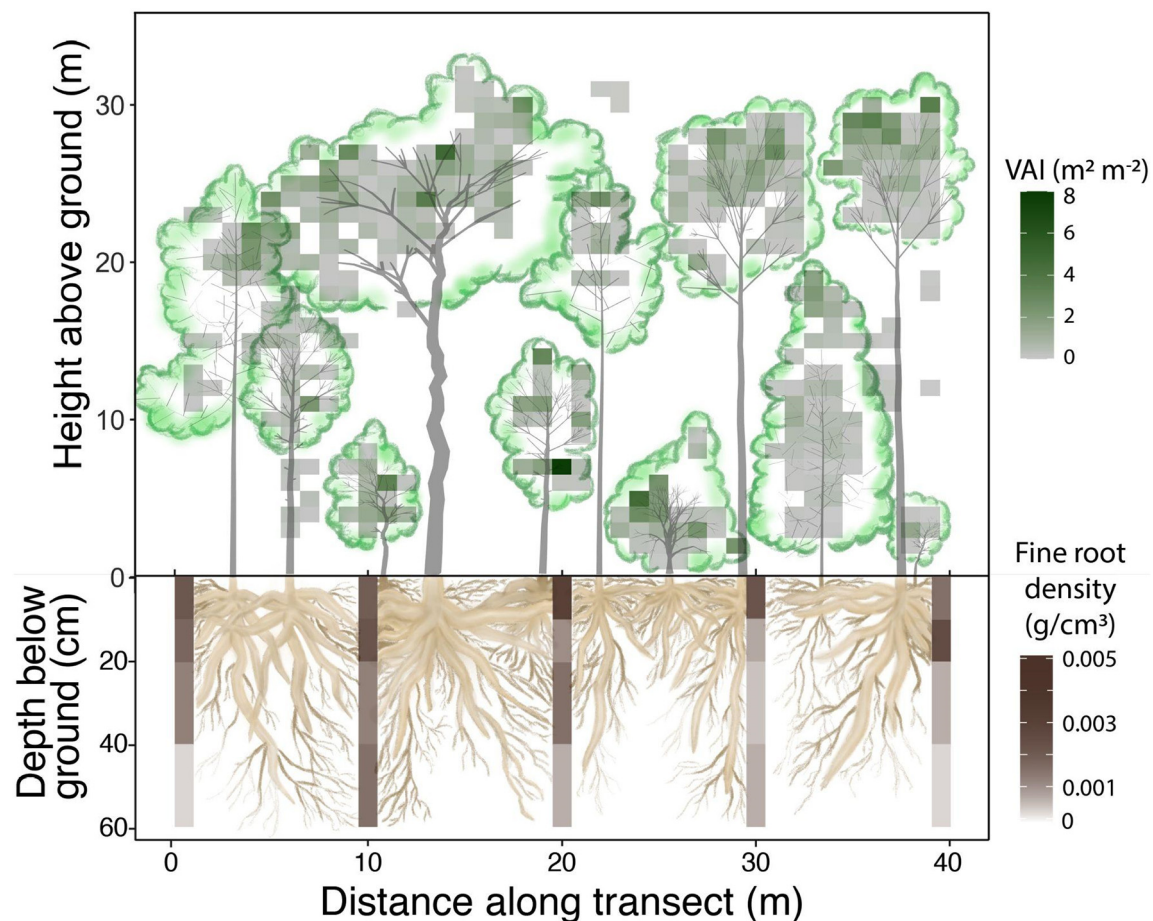


Fig. 1. Stylized cross-section of above- and belowground structural relationships, derived from terrestrial lidar and root excavations, respectively. Both approaches provide spatially explicit data on the vertical and horizontal (i.e. 2-dimensional) distribution of canopy or root biomass, permitting the derivation of above- and belowground measures of biomass density and complexity. This example depicts voxelized vegetation area index (VAI) and fine root mass density along a 40-m transect in the mixed deciduous and needleleaf (MIX) late successional stand. VAI voxels are to scale (1 m × 1 m) and root density (8-cm wide) voxels are proportionally exaggerated for illustrative clarity. Illustrations by Daulton White.

We assessed relationships between canopy and root structure, and determined whether soil respiration is linked to remotely sensed canopy structure through its influence on root spatial distribution and soil microclimatic factors with known mechanistic ties to soil CO₂ efflux. To accomplish this goal, we investigated forests across a glacially-formed landscape in northern Michigan spanning a range of aboveground structures shaped by successional development and disturbance (Scheuermann et al., 2018; Wales et al., 2020). Both successional processes and disturbance play primary roles in shaping within-landscape variation in vegetation structure (Gough et al., 2022); thus, our forested landscape containing a range of successional stages and disturbance histories serves as a useful setting for examining relationships between vegetation structure and function. Specifically, our objectives (O) were to: use forest successional and disturbance history gradients to establish and compare the variation in above- and belowground vegetation density and complexity across a forested landscape (O1); assess how aboveground structural measures relate to soil microclimatic and root structural parameters with known ties to soil respiration (O2); and determine whether canopy light absorption, soil microclimate, and root structure mediate relationships between canopy structure and soil respiration (O3). Our corresponding hypotheses (H) were: above and belowground stand-scale structural properties vary similarly across successional and disturbance gradients (Hardiman et al., 2017) (H1); canopy structural metrics summarizing heterogeneity in the distribution and density of vegetation in multiple dimensions (e.g., canopy rugosity) better predict spatial variation in mean soil temperature, moisture, and root structure than those summarizing vegetation density alone (e.g. vegetation area index) (Scheuermann et al., 2018) (H2); and canopy structure is linked to soil respiration through mediating biotic and abiotic pathways (H3).

2. Methods

2.1. Study site

Our study took place at the University of Michigan Biological Station (UMBS) in northern Lower Michigan, USA (45.558, -84.677). This landscape is covered by secondary forests, regrown following clear-cut harvesting and subsequent fires in the late 19th and early 20th centuries. With the goal of encompassing a breadth of above- and belowground structural variation, we conducted our study in two separate 100-yr chronosequences and three late successional forest stands spanning productivities, compositions, canopy complexities, and leaf area indices representative of forests throughout the broader Great Lakes - Laurentian Mixed Forest ecological province (Nave et al., 2017; Scheuermann et al., 2018; Wales et al., 2020). The two chronosequences differed by disturbance history at the time of stand establishment. The first chronosequence includes four, 1-ha “cut and burn” stands that were clear-cut and burned in 1936, 1954, 1980, or 1998; and the second consists of four “cut only” clear-cut (but not burned) 1-ha stands in 1911, 1952, 1972, or 1987. Early successional stands were populated mostly by bigtooth aspen (*Populus grandidentata*) and paper birch (*Betula papyrifera*), with mid-successional (~100-yr-old) stands transitioning to red oak (*Quercus rubra*) and red maple (*Acer rubrum*)

dominance. Late successional stands were > 130-yr-old and represented distinct plant functional types: deciduous broadleaf forests (DBF) dominated by *Q. rubra* and *A. rubrum*, evergreen needleleaf forest (ENF) dominated by *Pinus resinosa*, and a mix of both deciduous and needleleaf species (MIX; *Pinus strobus*, *P. resinosa*, *Q. rubra*, *P. grandidentata*). In each of the stands, sampling occurred in two or three, 0.1 ha plots ($n = 29$ total plots). Plots were considered the experimental unit of analysis.

2.2. Canopy and root structure

We used a portable below-canopy lidar (PCL) system equipped with an upward-facing, near-infrared laser to derive two categories of aboveground structure with strong ties to ecosystem functioning: vegetation area index (VAI) and canopy rugosity (Gough et al., 2019). Canopy data were collected at maximum leaf out in July 2021. VAI describes the number of leaf and woody vegetation layers present per unit ground area, while canopy rugosity quantifies the variation in VAI distribution horizontally and vertically (Table 1, Atkins et al., 2018b). We collected data along two, 40 m transects per plot; one running North-to-South and the other East-to-West. The PCL produces a vegetation hit-grid, mapping a cross-section of vegetation distribution throughout the canopy (Fig. 1). Plot-scale VAI and canopy rugosity were calculated from lidar data using the *forestr* R package (Atkins et al., 2018b). Details on PCL construction, operation, and other PCL-derived canopy traits can be found in an array of publications (Parker et al., 2004; Hardiman et al., 2011; Atkins et al., 2018b; Gough et al., 2020).

Root structure was derived from 2-dimensional belowground sampling conducted along the same transects sampled via PCL throughout July 2021 (Fig. 1, Table 1). We generated measures of fine root density and complexity that were similar to those derived for the canopy, but exact analogs of root and canopy structure were not possible given differences in above and belowground sampling resolutions (m² canopy hit grid vs 10–20 cm soil increments), dimensions (e.g., height and depth), and approaches (e.g., mass vs area). Roots were collected from four soil depths (0–10 cm, 10–20 cm, 20–40 cm, 40–60 cm) using a beveled steel conduit pipe with a 7 cm internal diameter. Sampling to this depth captures >90 % fine roots in our soils (He et al., 2013). Collection took place every 10 m along each transect (Fig. 1) in two plots per stand ($n = 22$ plots) producing a study-wide sample size of 198 vertical cores made up of 792 total soil increments. Each soil increment was sieved (using 2-mm mesh) for roots, roots were rinsed and oven dried, and then separated into fine (< 2 mm diameter) and coarse (> 2 mm diameter) pools before weighing. We retained fine roots and discarded coarse roots for analysis because of the former's high metabolic activity and predominant influence over soil CO₂ efflux (Desrochers et al., 2002). A subsample of roots from each soil depth increment in each stand was ashed in a muffle furnace at 500 °C for 12 h to adjust for mineral content. We found no statistical difference in mineral content by stand (ANOVA: $F = 0.88$, $p = 0.56$) or depth (ANOVA: $F = 2.34$, $p = 0.09$) and, therefore, applied a standard adjustment of the site-averaged 29 % mineral content to all root samples. Fine root mass density (Zhou and Shangguan, 2007) was calculated as grams per cubic centimeter of soil for each increment, averaged by column, then averaged across each

Table 1

Descriptions and sources of above- and belowground vegetation structure derived from portable below-canopy lidar aboveground and root excavations at multiple soil depth increments.

	Structural category	Unit	Description	References
Aboveground				
Canopy Rugosity	Complexity	m	Ratio of VAI variance in horizontal and vertical directions	Hardiman et al., 2011
Vegetation Area Index (VAI)	Density	dimensionless	Mean of column summed vegetation area index	Atkins et al., 2018b
Belowground				
Fine Root Complexity	Complexity	g/cm ³	Ratio of fine root mass density variance in horizontal and vertical directions	This study, modified from Hardiman et al., 2011
Fine Root Mass Density	Density	g/cm ³	Mean of column averaged fine root mass per unit soil volume	Zhou and Shangguan, 2007

plot. We calculated fine root complexity from vertical and horizontal root mass density distributions, modifying the Hardiman et al. (2011) formula of canopy rugosity (Hardiman et al., 2011):

$$\text{Fine Root Complexity} = (\sigma (\sigma [\text{fine root mass density}]_z)_x) \quad (1)$$

where z is the vertical depth increment, x is the horizontal transect sampling location, and σ is standard deviation.

2.3. Soil respiration and microclimate

In situ growing-season soil respiration was collected during the same year as root and canopy structure sampling, on July 26–28, 2021, using a LiCOR-6400 paired with a LI-6400-09 soil CO₂ flux chamber at 5 soil collars per plot. Each collar is a 10 cm diameter PVC pipe that sits 3–5 cm deep into the soil and was installed in 2014. Collars were arranged 3 m, 6 m, 9 m, 12 m, and 15 m in a spiral starting northward around and away from plot center to allow for representative sampling of the plot. Chamber conditions were set to 400 ± 10 ppm CO₂ and two measurements of CO₂ efflux were recorded at each collar and averaged for analysis. Alongside respiration, soil moisture (in the top 20 cm depth) and temperature (in the top 7 cm depth) were collected 2 cm away from each collar using a Campbell Hydrosense II and built-in LI-6400 thermocouple, respectively. Analyses were restricted to soil microclimate and respiration collected once in 2021 to align with root and canopy structure characterized in the same growing season; however, all data were comparable to averages from repeated measurements following the same methods at the same plots and collars during the prior year, 2020 (Clay et al., 2022).

Light absorption was estimated as the fraction of photosynthetically active radiation (fPAR) absorbed by the canopy. In each plot, fPAR was measured using an AccuPAR LP-80 along the same 40-m perpendicular transects used to sample canopy and root structure. Below canopy PAR observations were taken 1 m above the forest floor approximately every 1 m along the transect, then compared to open-sky, above-canopy reference measurements. All light data were recorded within two hours of solar noon on cloudless days after full leaf-out, in late June or early July 2021.

2.4. Statistical analysis by objective (O)

2.4.1. O1: Variation in canopy and root structure across successional and disturbance gradients

To establish and compare the range of structural variation above- and belowground in chronosequence and late successional stands, we used linear regression and ANOVA, respectively ($\alpha = 0.05$). For all analyses, plots ($n = 29$ for canopy data, $n = 22$ for root data) were considered the experimental unit, with stand-level means and standard errors presented in corresponding figures. Simple linear regression was used to determine whether changes over time in the cut-only and cut-and-burn chronosequences were significant ($\alpha = 0.05$) and slope differences assessed by comparing 95 % parameter confidence intervals. Late successional stands serve as less-disturbed references, representative of age and community structures that would be common in the absence of stand-replacing disturbances a century ago (Nave et al., 2017); thus, we compared these late successional references with the oldest chronosequence stands via ANOVA with Tukey's HSD pairwise comparisons. Assumptions of linearity, normality, and homogeneity of variance were checked using visual inspection of scatter, Q-Q, and residual plots using the *stats* package in base R (v4.1.2; R Core Team, 2021). Canopy structural relationships across these successional gradients are presented and interpreted elsewhere (Scheuermann et al., 2018; Wales et al., 2020). Here, we present for the first time surveys of root structure alongside canopy structure at our site.

2.4.2. O2: bivariate relationships between canopy structure, root structure, and soil microclimate

We used simple linear regression to assess bivariate relationships between canopy rugosity or VAI and soil temperature, soil moisture, fine root mass density, and fine root complexity ($\alpha = 0.05$). Assumptions of linearity, normality, and homogeneity of variance were checked using visual inspection of scatter, Q-Q, and residual plots in R.

2.4.3. O3: Multivariate pathways from canopy structure to soil respiration

To provide an integrative assessment of hypothesized biotic and abiotic interactions mediating canopy structure-soil respiration interactions, we compared separate path analyses that included canopy rugosity or VAI as starting explanatory variables. We omitted plots from our analysis for which roots were not collected, leaving a sample size of 22, and log-transformed fine root mass density data to meet homogeneity of variance requirements. Path analyses were evaluated by confirmatory factor analysis and goodness-of-fit metrics were calculated using the *sem* package in R (Fox, 2006). To balance model complexity with our limited sample size, we only retained variables in our path analysis that were significantly correlated with VAI or canopy rugosity in O2. We first ran full models containing all pathways hypothesized a priori to link canopy structure and soil respiration, incorporating mechanistically-grounded variables and interactions supported by prior literature, but not previously tested in a multivariate framework (Fig. A.1). We included fPAR in our model selection because of its close association with both canopy structure (Atkins et al., 2018a) and soil microclimate (Gálhidy et al., 2006; Hardwick et al., 2015). We then reduced models by retaining variables with $P < 0.1$, applying a slightly more conservative alpha than the conventional default of 0.15 used in multivariate model selection because of our small sample size (Steyerberg, 2009). We compared full and reduced models using Akaike information criterion (AIC) and sample-size adjusted Bayesian information criterion (SABIC) scores.

3. Results

3.1. O1: Canopy and root structure over succession and disturbance histories

Aboveground structure was more dynamic over successional timescales than belowground structure. Canopy rugosity and VAI increased similarly in the two chronosequences over ~100 years of stand development (Fig. 2), a trend that corroborates prior findings at our site (Scheuermann et al., 2018). There is some evidence ($R^2 = 0.14, p = 0.06$) of increasing VAI from 5.1 to 6.9 with stand age (Fig. 2a). Pairwise comparisons suggest that the VAI of the oldest cut and burn stand was similar that of the ENF stand, the oldest cut only stand was similar to the DBF stand, and the MIX stand was similar to all other stands (Fig. 2a). Canopy rugosity was much more dynamic, increasing four-fold from 3.1 m to 12.7 m ($R^2 = 0.74, p < 0.001$) over nearly a century (Fig. 2b). Late successional stands had higher canopy rugosity than the oldest cut only and cut and burn stands, around 30 m ($p < 0.001, F = 13.94$) (Fig. 2b).

In contrast to aboveground structure, there were no significant changes over time or among secondary and late successional stands in root mass density or complexity (Fig. 2). Fine root mass density varied from ~0.002 g/cm³ to ~0.004 g/cm³ among stands and displayed no significant trend through succession ($p = 0.97$) or differences between oldest chronosequence and late succession stands ($p = 0.47, F = 1.26$) (Fig. 2c). Similarly, fine root complexity, averaging 0.002 g/cm³, exhibited no significant successional trend ($p = 0.20$) or differences between the oldest secondary and late successional stands ($p = 0.49, F = 1.19$) (Fig. 2d).

3.2. O2: Bivariate relationships between canopy structure, root structure, and soil microclimate

Canopy rugosity was more closely correlated with belowground biotic and abiotic factors than VAI (Fig. 3). Canopy rugosity exhibited negative

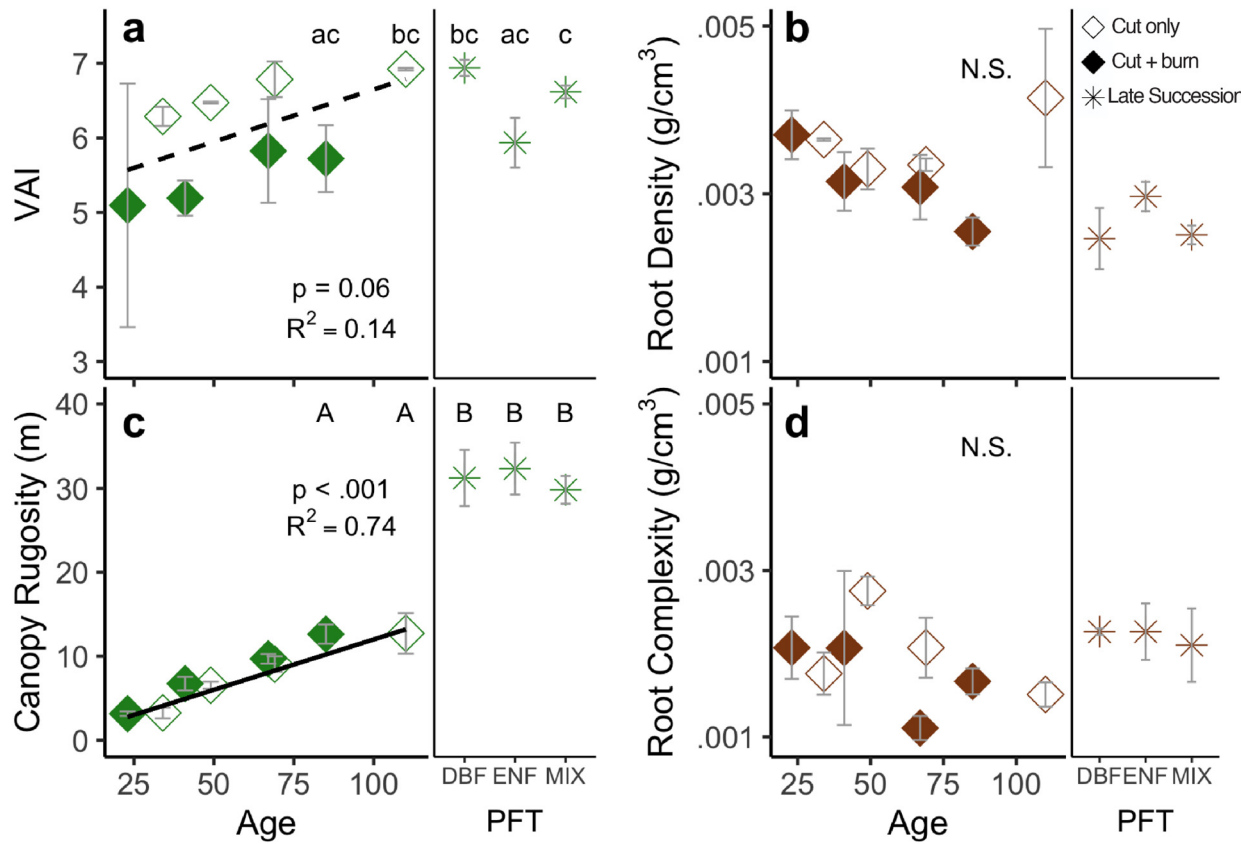


Fig. 2. Side-by-side comparisons of above- and belowground measures of vegetation density (a, b) and complexity (c, d) by stand age for cut only and cut and burn chronosequences and by dominant plant functional type (PFT) for late successional stands. Plant functional types represented are deciduous broadleaf (DBF), evergreen needleleaf (ENF), and mixed deciduous and needleleaf (MIX). The dashed trendline illustrates a common (for both chronosequences) marginally significant ($P < 0.1$) relationship and the solid line a shared significant ($P < 0.01$) relationship. P and adjusted R^2 values are presented for significant linear models. Letters indicate significant pairwise differences among late successional and the oldest chronosequence stands. Means \pm SE, VAI—vegetation area index, N.S.—not significant.

bivariate relationships with fine root mass density ($R^2 = 0.36, p = 0.002$) and soil temperature ($R^2 = 0.25, p = 0.004$), and a positive relationship with soil moisture ($R^2 = 0.26, p = 0.003$) (Fig. 3). VAI was positively correlated with soil moisture ($R^2 = 0.22, p = 0.006$), but not soil temperature ($p = 0.29$) or fine root mass density ($p = 0.39$) (Fig. 3). Fine root complexity did not correlate with either VAI ($p = 0.49$) or canopy rugosity ($p = 0.73$), and thus was not retained as an explanatory variable for multivariate path analyses.

3.3. O3: Multivariate pathways from canopy structure to soil respiration

Path analysis revealed that canopy rugosity was more strongly coupled to soil respiration than VAI through process-mediating biotic and abiotic factors (Fig. 4, Table 2). Canopy rugosity was biotically linked to soil respiration through a direct, positive correlation as well as an indirect pathway mediated by fine root density (Fig. 4a). The fine root-mediated pathway suggests a moderately negative correlation between canopy rugosity and fine root mass density ($R = -0.67$, Fig. 3a) and a subsequent positive relationship between root mass density and soil respiration ($r = 0.64$, Fig. 4a). Canopy rugosity explained soil moisture variation through two positively correlated relationships; one direct ($R = 0.55$) and one light absorption-mediated ($R = 0.45$ and 0.29, Fig. 4a). These relationships with soil moisture served as an abiotic link from canopy rugosity to soil respiration ($R = -0.57$, Fig. 4a). Although a significant relationship between canopy rugosity and soil temperature emerged in bivariate analysis (O2, Fig. 3b), soil temperature was not retained as a significant mediator between canopy

rugosity and soil respiration in a multivariate context (Fig. 4a). In contrast to the more statistically robust pathways in our reduced canopy rugosity model, VAI did not directly relate to soil respiration and significant covariances existed among VAI, soil temperature, and fine root mass density (Fig. 4b). However, VAI was coupled to soil moisture through similarly moderate direct and indirect fPAR-mediated pathways. Overall, the highest-ranking canopy rugosity multivariate model (Table 2) incorporating biotic and abiotic factors accounted for 43 % of plot-scale variation in soil respiration, while the highest-ranking VAI model accounted for 35 %.

4. Discussion

Our results demonstrate that forest canopy complexity and, to a lesser extent, VAI are integrators of mechanistically-grounded biotic and abiotic drivers of soil respiration at our site. Canopy rugosity, one of many newer metrics of canopy structural complexity (Atkins et al., 2018b; Ehbrecht et al., 2016), strongly predicts the spatio-temporal dynamics of above-ground vegetation and production (Scheuermann et al., 2018; Atkins et al., 2018a; Gough et al., 2019). Our findings show that similar predictive capabilities may extend to soil respiration, a more poorly constrained C-cycling process (Bond-Lamberty et al., 2020), through canopy complexity's effects on fine root density, canopy light interception, and soil moisture. If applicable to other sites and ecosystems, our findings could provide a mechanistically-informed basis for more broadly inferring stand-level variation in soil respiration from remotely sensed above-ground vegetation complexity.

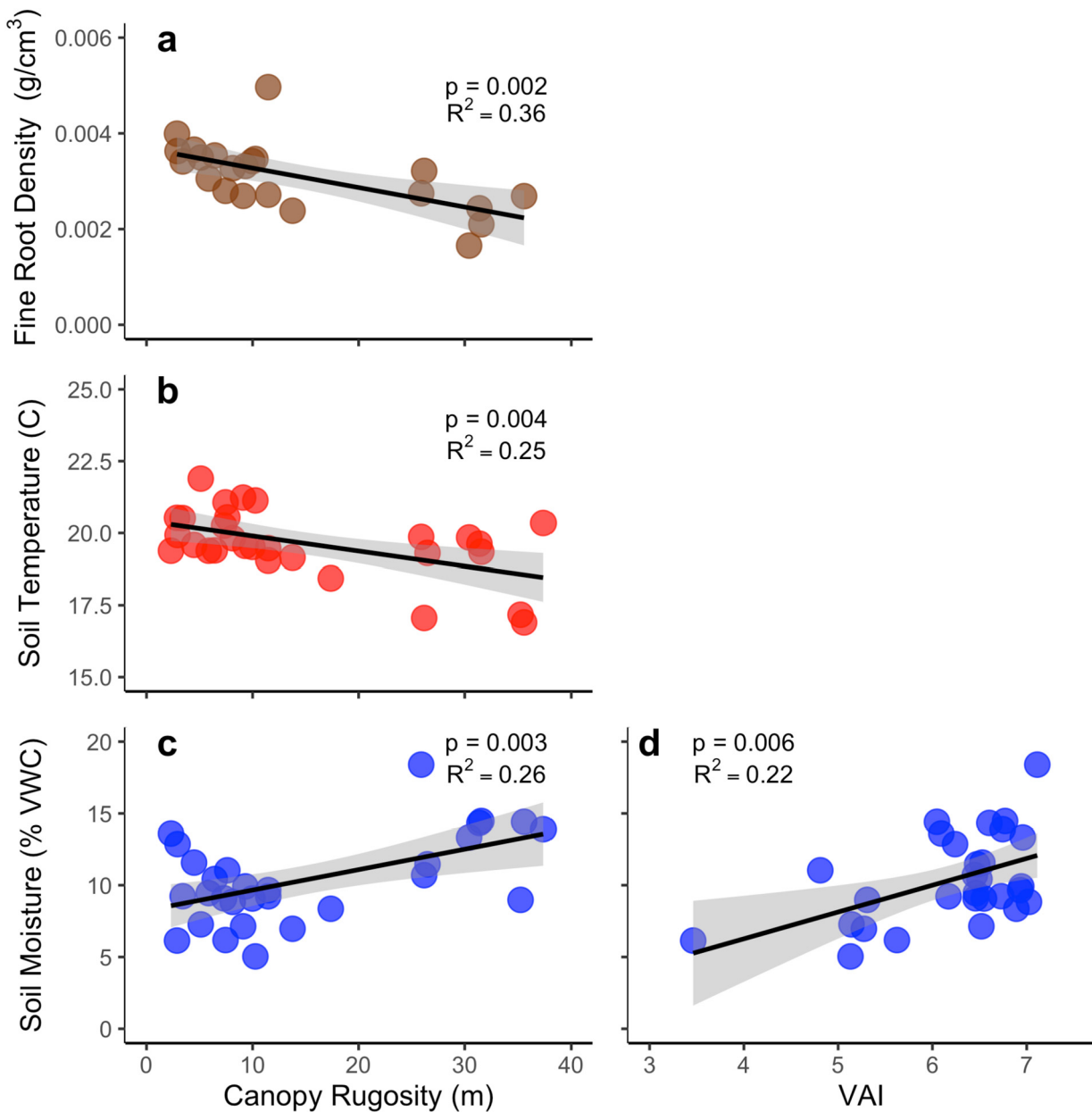


Fig. 3. Canopy rugosity in relation to mean plot fine root mass density (a), soil temperature (b), and soil moisture (c) and vegetation area index (VAI) in relation to soil moisture (d). Solid lines denote significant linear relationships and gray shaded areas illustrate 95 % confidence intervals. VWC—volumetric water content. Non-significant ($P > 0.05$) relationships are not shown.

We found that canopy rugosity was a more robust predictor of soil respiration than VAI, with this canopy complexity metric exhibiting stronger ties to known biotic and abiotic drivers of soil C fluxes. While our analysis is among the first to elucidate interconnected biotic and abiotic pathways coupling canopy complexity and soil respiration, assessments of individual pathways offer support for our findings. For example, our analysis shows that canopy complexity is correlated with soil microclimate through its effects on light transmission. Complex forest canopies absorb more light (Ishii et al., 2004; Atkins et al., 2018a), limiting the energy reaching the forest floor and reducing evaporation from soils (Flerchinger and Pierson, 1991; Forrester et al., 2012). Taller, denser, and more complex canopies also maintain higher levels of interior humidity and reduce vertical mixing of within-canopy air (Renaud et al., 2011; von Arx et al., 2012), which may further limit soil evaporative losses. In addition, complex canopies use resources – including water – more efficiently to drive production

(Hardiman et al., 2011; Gough et al., 2019; Murphy et al., 2022), suggesting that more complex, higher VAI forests may, counter-intuitively, lose less water through evapotranspiration than those with lower complexity and VAI. In our analysis, the abiotic pathways connecting VAI and canopy complexity to soil respiration were similar, but stronger relationships with canopy rugosity reinforce other site-to-biome studies that suggest canopy complexity is more closely related to canopy light absorption than vegetation and leaf area indices (Atkins et al., 2018a; Gough et al., 2019). However, the weaker VAI-soil respiration relationship in our study could arise from a quantitatively narrower range of VAI relative to canopy rugosity, highlighting the importance of extending similar analyses to a range of sites varying in canopy complexity and leaf/vegetation area.

Spatio-temporal patterns of above- and belowground vegetation structure at our site are similar to those of other forests; however,

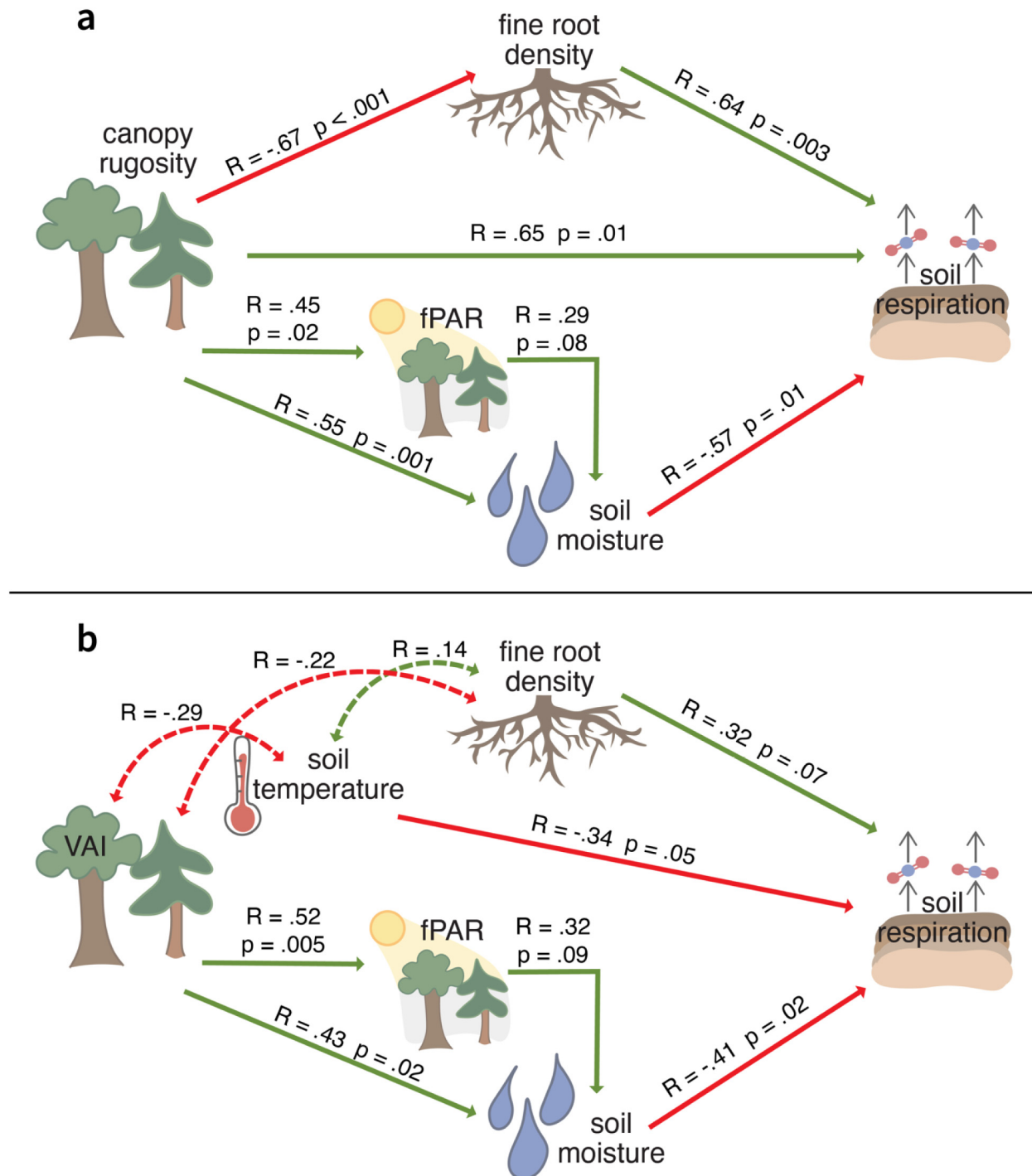


Fig. 4. Path diagrams illustrating direct and indirect biotic and abiotic relationships coupling soil respiration to canopy rugosity (a) and vegetation area index (VAI, b). Respective correlation coefficients and *p*-values for best-fitting VAI (AIC = 104, SABIC = 86) and canopy rugosity (AIC = 88, SABIC = 66) models presented. Arrow color indicates direction of correlation where positive correlations are green and negative correlations are red. Dashed and curved lines illustrate significant covariance between variables.

we did not observe stand-scale correlations between analogous above- and belowground vegetation density or complexity measures. Our results reinforce findings that the successional development of canopy structure may be more dynamic than that of root structure (Cavelier et al., 1996). However, a complete lack of spatial correspondence between above- and belowground structure is at odds with some prior observations demonstrating spatial correlation between root and

canopy gaps (Ostertag, 1998; Suchewaboripont et al., 2015; Taskinen et al., 2003; Hardiman et al., 2017). A successional divergence of above and belowground measures of vegetation density and complexity indicates vertical fine root densities and distributions are highly conserved over time at our site, and consequently decoupled from the dynamic changes in canopy complexity. In our closed-canopy forest stands, more conserved fine root structures may reflect

Table 2

Summary of model goodness-of-fit statistics for multivariate pathways (illustrated in Fig. 4) including chi-square estimation, root mean square error approximation (RMSEA), confirmatory factor index (CFI), standardized root mean square residual (SRMR), Akaike information criterion (AIC) scores, and sample-size adjusted Bayesian information criterion (SABIC) scores. The best-fitting model is highlighted in green. VAI—vegetation area index.

Canopy trait	χ ²		RMSEA		CFI	SRMR	AIC	SABIC
	Estimate	P-value	Estimate	P-value				
Canopy rugosity reduced model	1.8	0.61	<.001	0.64	1.00	0.04	88	66
VAI reduced model	7.7	0.26	0.11	0.29	0.927	0.12	104	86
Canopy rugosity full model	5.6	0.34	0.08	0.38	0.986	0.07	155	125
VAI full model	6.8	0.23	0.13	0.26	0.922	0.11	178	148

the relatively fixed vertical taper and depth of rooting in many temperate forests (Zhou and Shangguan, 2007), with most fine roots contained within the top 20 cm of mineral soil in all of our stands. In contrast, aboveground vegetation height, which was variable among our forest stands (Scheuermann et al., 2018), places a primary constraint on canopy complexity because taller canopies contain more space within which to construct heterogeneous vegetation arrangements (Gough et al., 2020). We note, however, that variation in fine root density and distribution could be limited at our site because of relatively homogeneous soils (Gale and Grigal, 1987), suggesting that broader spatial-scale comparisons of canopy-root structural relationships across soil textures, structures, and densities could yield different results.

Although not above- and belowground structural analogs, we found that fine root density decreased as canopy rugosity increased (Fig. 3), possibly because canopy complexity is positively correlated with site productivity (Gough et al., 2019) and more productive forests invest relatively less in fine root production (Nadelhoffer, 2000). Forests allocating less in belowground biomass, in turn, may exhibit lower soil autotrophic respiration (Litton et al., 2007). Interpreting canopy rugosity-root density relationships in the context of our path analysis, fewer fine roots in complex and productive forests appear to be an ecologically plausible mediating pathway connecting canopy rugosity—but not VAI—to soil respiration.

While many of the pathways connecting canopy structure to soil respiration are supported by prior knowledge, some interactions among these pathways are less straightforward. For example, other studies from our site show that more complex stands have equal or lower soil respiration rates than less complex stands (Lieberman et al., 2017; Clay et al., 2022), which is counter to the direct, positive relationship between canopy complexity and soil respiration in our multivariate analysis. In this context, the direct pathway that we observed from canopy rugosity to soil respiration could be caused by complexity's positive influence on C fixation and production (Hardiman et al., 2011; Gough et al., 2019), factors that limit stand-scale soil respiration (Bond-Lamberty et al., 2004). More complex canopies sequester more C (Hickey et al., 2019; Gough et al., 2019) and, in doing so, may allocate proportionally more

photosynthate to belowground metabolism (Högberg et al., 2001). This pathway could also indicate the effect of additional direct and/or indirect variables, such as soil nutrient status, which also vary across the study landscape and are not mutually exclusive to other variables and pathways (Hofmeister et al., 2019; Nave et al., 2017). Spatial variation of soil nutrients in particular is associated with canopy complexity-soil respiration relationships in ecosystems with similar vegetation types (Suchewaboripont et al., 2015). In addition, we found a negative relationship between soil moisture and respiration in a multivariate context, which is counter to experiments that show water limitations constrain root and microbial metabolic activity and, consequently, respiration rates (Orchard and Cook, 1983; Curiel Yuste et al., 2007). A negative relationship between soil moisture and respiration has been observed previously at our site (Curtis et al., 2005; Clippard et al., 2022), and could reflect the co-variance of temperature and moisture, rather than the direct influence of water availability on metabolic processes, with cooler soils generally containing more water but respiring less. Future inclusion of additional canopy structure-soil respiration mediating factors may further resolve the drivers connecting canopy complexity and soil respiration, while increasing the overall predictive power and mechanistic understanding of our multivariate path model.

While our study provides new mechanistic insight into the connections between forest canopy structure and soil respiration, we note several limitations and opportunities for future analysis. First, our sample size is modest and our analysis limited to forest ecosystems of the upper Great Lakes region. Additional work is required to determine whether the patterns that we observed extend to other forested regions, particularly in advance of inferring soil respiration more broadly via the remote sensing of canopy structure. Secondly, our models, while informed by a priori mechanistic understanding, are statistical and thus correlative, and they are not inclusive of all known biotic and abiotic drivers of soil respiration. For example, our analyses did not consider microbial properties and processes, edaphic factors such as soil texture or nitrogen availability, or site productivity, all of which may affect vegetation structure and soil respiration (Gale and Grigal, 1987; Nadelhoffer, 2000; Curiel Yuste et al., 2007). Thirdly, our assessment of canopy structure-soil respiration

relationships focused on only one phenological period, peak leaf out, and our focus was on instantaneous rather than cumulative soil respiration fluxes. Relationships between canopy structure and soil respiration may vary seasonally, perhaps decoupling, as processes such as dormancy overwhelm mediating influences of microclimate outside of the growing season (Villegas et al., 2010). Finally, additional work is required to elucidate the spatio-temporal scales of structure-function coherence. Soil respiration exhibits relatively high spatio-temporal variation within forest stands and across seasons (Lavigne et al., 2004), while canopy structural features are integrative, representative of larger-scale forest properties and relatively stable during peak leaf-out (Hardiman et al., 2017). Thus, the ecologically-relevant scale(s) of coherence between canopy structure and C cycling processes require further investigation, particularly in advance of efforts to predict soil respiration at larger spatial scales and across seasons. Despite these limitations, our findings provide a mechanistically-informed foundation upon which to advance understanding of forest canopy structure-soil respiration relationships, a critical first step to developing more comprehensive models that can be used to remotely sense belowground C cycling processes from above-ground vegetation properties.

5. Conclusions

Our findings provide a mechanistically-informed basis for the remote sensing of soil respiration from lidar-derived canopy structure, building from analyses that established relationships between soil respiration and field observations or qualitative assessments of canopy structure (Cai et al., 2021; Ma et al., 2014; Forrester et al., 2012; Bréchet et al., 2011; Katayama et al., 2009), or remotely sensed reflectance-based vegetation indices (Xiao et al., 2019). Our results suggest that new and emergent (Shiklomanov et al., 2020) lidar-derived canopy complexity measures can robustly integrate the effects of biotic and abiotic drivers of soil respiration. Advancing mechanistic understanding of the relationships between canopy and belowground processes remains a critical frontier, essential to the refinement and development of the next-generation indices of ecosystem functioning (Cavender-Bares et al., 2022). If applicable to other forests, linkages between canopy rugosity and soil respiration could permit broader spatial-scale inference of belowground biogeochemical processes from the ground-to-spaceborne remote sensing of aboveground vegetation structure. Such evaluation of canopy complexity-soil biogeochemical interactions

across sites is now feasible using open data provided by lidar-equipped aircraft and satellite platforms (Beland et al., 2019; Shiklomanov et al., 2020; Gough et al., 2022) and ecological networks, including FLUXNET, which freely provide C fluxes for a diversity of ecosystems (Baldocchi et al., 2001).

CRediT authorship contribution statement

Laura J. Hickey: Conceptualization; Data curation; Formal analysis; Investigation; Methodology; Project administration; Supervision; Validation; Visualization; Writing - original draft. Lucas E. Nave: Funding acquisition; Writing - review & editing. Knute J. Knadelhoffer: Funding acquisition. Cameron Clay: Data curation; Investigation; Project administration; Validation; Writing - review & editing. Alexandra I Marini: Investigation. Christopher M. Gough: Conceptualization; Funding acquisition; Methodology; Supervision; Resources; Writing - original draft.

Code and data availability

All code and data used to perform statistical analysis and generate figures are available via Figshare: <https://doi.org/10.6084/m9.figshare.19782403> and an R Project at <https://doi.org/10.6084/m9.figshare.19782397>.

Data availability

I have included links to code and data availability in the body of my manuscript lines 508-510

Declaration of competing interest

The authors declare that they have no known competing financial interests or personal relationships that could have appeared to influence the work reported in this paper.

Acknowledgements

This work was supported by the National Science Foundation, Division of Environmental Biology, through awards 1353908 and 1856319. We thank the University of Michigan Biological Station for logistical support.

Appendix A

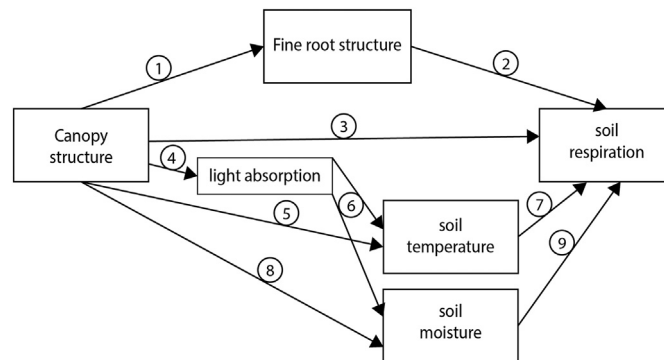


Fig. A.1. Hypothesized pathways linking canopy structure (i.e. vegetation area index or canopy rugosity) to soil respiration. Individual paths (i.e. connecting two variables) were informed a priori from published literature. Our conceptual and statistical frameworks consider these interactions simultaneously and in an integrative context. The number on each pathway corresponds with previous findings as follows: 1. Hopkins et al., 2013, Suchewaboripont et al., 2015, Hardiman et al., 2017. 2. Litton et al., 2007, Suchewaboripont et al., 2015, Wang et al., 2017. 3. Tanaka and Hashimoto, 2006, Katayama et al., 2009, Shi et al., 2016, D'Andrea et al., 2020, Cai et al., 2021. 4. Ishii et al., 2004, Atkins et al., 2018a. 5. McCarthy and Brown, 2006, Forrester et al., 2012. 6. Gálhidy et al., 2006, Hardwick et al., 2015. 7. Raich and Schlesinger, 1992. 8. McCarthy and Brown, 2006, Forrester et al., 2012, Cai et al., 2021. 9. Raich and Schlesinger, 1992.

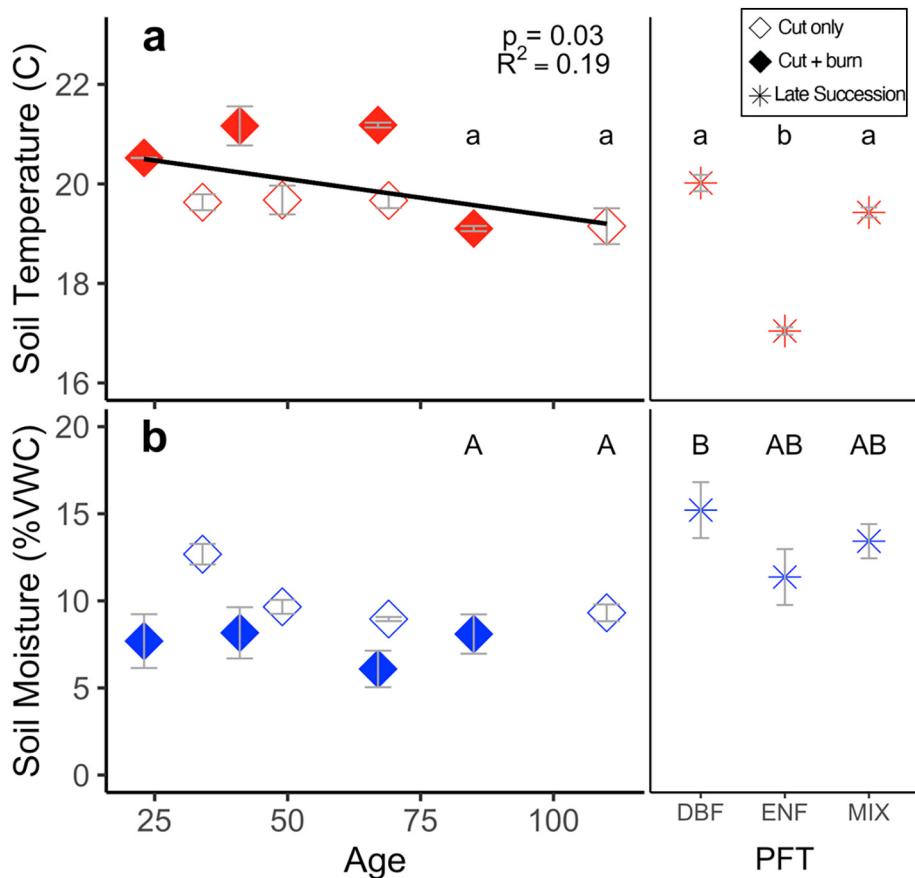


Fig. A.2. Mean soil temperature (a) and soil moisture (as volumetric water content or VWC, b) \pm SE by stand age for cut only and cut and burn chronosequences and by dominant plant functional type (PFT) for late successional stands. Plant functional types represented are deciduous broadleaf (DBF), evergreen needleleaf (ENF), and mixed deciduous and needleleaf (MIX). The solid line in panel a denotes a shared significant ($P < 0.05$) relationship. P and adjusted R^2 values are presented for significant linear models. Letters indicate significant pairwise differences among late successional and the oldest chronosequence stands.

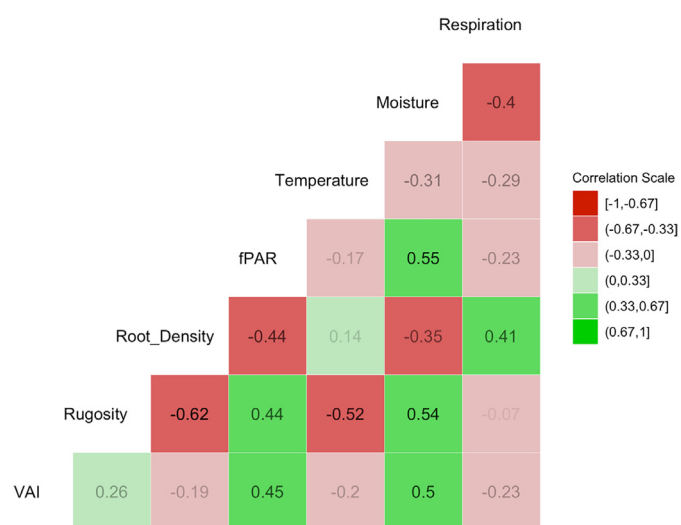


Fig. A.3. Correlation matrix of the structural, microclimatic, and soil respiration variable(s) evaluated via bivariate analysis for O2 and retained for multivariate analysis in O3. Green and red indicate positive and negative signs of correlation, respectively. Contrast and shading represent the strength of the correlation where strongest ($|R| > 0.66$) correlations are darker and weakest ($|R| < 0.33$) correlations are lighter.

References

von Arx, Georg, Dobbertin, Matthias, Rebetez, Martine, 2012. Spatio-temporal effects of forest canopy on understory microclimate in a long-term experiment in Switzerland. *Agric. For. Meteorol.* 166–167. <https://doi.org/10.1016/j.agrformet.2012.07.018>.

Atkins, J.W., Fahey, R.T., Hardiman, B.H., Gough, C.M., 2018a. Forest canopy structural complexity and light absorption relationships at the subcontinental scale. *J. Geophys. Res. Biogeosci.* 123 (4). <https://doi.org/10.1002/2017JG004256>.

Atkins, Jeff W., Bohrer, Gil, Fahey, Robert T., Hardiman, Brady S., Morin, Timothy H., Stovall, Atticus E.L., Zimmerman, Naupaka, Gough, Christopher M., 2018b. Quantifying vegetation and canopy structural complexity from terrestrial LiDAR data using the forestr package. *Methods Ecol. Evol.* 9 (10). <https://doi.org/10.1111/2041-210X.13061>.

Baldocchi, Dennis, Falge, Eva, Gu, Lianhong, Olson, Richard, Hollinger, David, Running, Steve, Anthony, Peter, et al., 2001. FLUXNET: a new tool to study the temporal and spatial variability of ecosystem-scale carbon dioxide, water vapor, and energy flux densities. *Bull. Am. Meteorol. Soc.* 82 (11). [https://doi.org/10.1175/1520-0477\(2001\)082<2415:FLXNT>2.3.CO;2](https://doi.org/10.1175/1520-0477(2001)082<2415:FLXNT>2.3.CO;2).

Beland, Martin, Parker, Geoffrey, Ben Sparrow, D., Harding, L., Chasmer, Phinn, Stuart, Antonarakis, Alexander, Strahler, Alan, 2019. On promoting the use of Lidar systems in forest ecosystem research. *For. Ecol. Manag.* 450 (October), 117484. <https://doi.org/10.1016/J.FORECO.2019.117484>.

Bond-Lamberty, Ben, Wang, Chuanhua, Gower, Stith T., 2004. A global relationship between the heterotrophic and autotrophic components of soil respiration? *Glob. Chang. Biol.* 10 (10). <https://doi.org/10.1111/j.1365-2486.2004.00816.x>.

Bond-Lamberty, Ben, Christianson, Daniella S., Malhotra, Avni, Pennington, Stephanie C., Sih, Debjani, AghaKouchak, Amir, Anjileli, Hassan, et al., 2020. COSORE: a community database for continuous soil respiration and other soil-atmosphere greenhouse gas flux data. *Glob. Chang. Biol.* 26 (12), 7268–7283. <https://doi.org/10.1111/GCB.15353>.

Bréchet, Laëtitia, Ponton, Stéphane, Almérás, Tancrède, Bonal, Damien, Epron, Daniel, 2011. Does spatial distribution of tree size account for spatial variation in soil respiration in a tropical forest? *Plant and Soil* 347 (1). <https://doi.org/10.1007/s11104-011-0848-1>.

Cai, Yihan, Nishimura, Takahiro, Ida, Hideyuki, Hirota, Mitsuhiro, 2021. Spatial variation in soil respiration is determined by forest canopy structure through soil water content in a mature beech forest. *For. Ecol. Manag.* 501 (December). <https://doi.org/10.1016/J.FORECO.2021.119673>.

Cavelier, Jaime, Estévez, Jaime, Arjona, Beatriz, 1996. Fine-root biomass in three successional stages of an Andean cloud forest in Colombia. *Biotropica* 28 (4). <https://doi.org/10.2307/2389059>.

Cavender-Bares, Jeannine, Schweiger, Anna K., Gamon, John A., Gholzadeh, Hamed, Helzer, Kimberly, Lepš, Jaroslav, Madritch, Michael D., et al., 2022. Remotely detected aboveground plant function predicts belowground processes in two prairie diversity experiments. *Ecol. Monogr.* 92 (1), e01488. <https://doi.org/10.1002/ECM.1488>.

Clay, Cameron, Nave, Luke, Nadelhoffer, Knute, Vogel, Christopher, Propson, Brooke, den Uyl, John, Hickey, Laura J., Barry, Alexandra, Gough, Christopher M., 2022. Fire after clear-cut harvesting minimally affects the recovery of ecosystem carbon pools and fluxes in a great lakes forest. *For. Ecol. Manag.* 519 (September), 120301. <https://doi.org/10.1016/J.FORECO.2022.120301>.

Clippard, E.A., Haruna, S.I., Curtis, P.S., et al., 2022. Decadal forest soil respiration following stem girdling. *Trees*. <https://doi.org/10.1007/s00468-022-02340-x>.

Curiel Yuste, J., Baldocchi, D.D., Gershenson, A., Goldstein, A., Misson, L., Wong, S., 2007. Microbial soil respiration and its dependency on carbon inputs, soil temperature and moisture. *Glob. Chang. Biol.* 13 (9), 2018–2035. <https://doi.org/10.1111/j.1365-2486.2007.01415.x>.

Curtis, P.S., Vogel, C.S., Gough, C.M., Schmid, H.P., Su, H.B., Bovard, B.D., 2005. Respiratory carbon losses and the carbon-use efficiency of a northern hardwood forest, 1999–2003. *New Phytol.* 167 (2), 437–456. <https://doi.org/10.1111/j.1469-8137.2005.01438.x>.

D'Andrea, Ettore, Guidolotti, Gabriele, Scartazza, Andrea, de Angelis, Paolo, Matteucci, Giorgio, 2020. Small-scale forest structure influences spatial variability of belowground carbon fluxes in a mature Mediterranean beech forest. *Forests* 11 (3). <https://doi.org/10.3390/f11030255>.

Desrochers, Annie, Landhäusser, Simon M., Lieffers, Victor J., 2002. Coarse and fine root respiration in Aspen (*Populus tremuloides*). *Tree Physiol.* 22 (10). <https://doi.org/10.1093/treephys/22.10.725>.

Ehbrecht, Martin, Schall, Peter, Juchheim, Julia, Ammer, Christian, Seidel, Dominik, 2016. Effective number of layers: a new measure for quantifying three-dimensional stand structure based on sampling with terrestrial LiDAR. *For. Ecol. Manag.* 380. <https://doi.org/10.1016/j.foreco.2016.09.003>.

Flerchinger, G.N., Pierson, F.B., 1991. Modeling plant canopy effects on variability of soil temperature and water. *Agric. For. Meteorol.* 56, 3–4. [https://doi.org/10.1016/0168-1923\(91\)90093-6](https://doi.org/10.1016/0168-1923(91)90093-6).

Forrester, Jodi A., Mladenoff, David J., Gower, Stith T., Stoffel, Jennifer L., 2012. Interactions of temperature and moisture with respiration from coarse woody debris in experimental forest canopy gaps. *For. Ecol. Manag.* 265. <https://doi.org/10.1016/j.foreco.2011.10.038>.

Fox, J., 2006. Structural equation modeling with the sem package in R. *Struct. Equ. Model.* 13 (3), 465–486. https://doi.org/10.1207/s15328007sem1303_7.

Gale, M.R., Grigal, D.F., 1987. Vertical root distributions of northern tree species in relation to successional status. *Can. J. For. Res.* 17 (8). <https://doi.org/10.1139/x87-131>.

Gálhidy, László, Mihók, Barbara, Hagyó, Andrea, Rajkai, Kálmán, Standovár, Tibor, 2006. Effects of gap size and associated changes in light and soil moisture on the understorey vegetation of a Hungarian beech forest. *Plant Ecol.* 183 (1). <https://doi.org/10.1007/s11258-005-9012-4>.

Gough, Christopher M., Atkins, Jeff W., Fahey, Robert T., Hardiman, Brady S., 2019. High rates of primary production in structurally complex forests. *Ecology* 100 (10). <https://doi.org/10.1002/ecy.2864>.

Gough, Christopher M., Atkins, Jeff W., Fahey, Robert T., Hardiman, Brady S., LaRue, Elizabeth A., 2020. Community and structural constraints on the complexity of eastern North American forests. *Glob. Ecol. Biogeogr.* 29 (12). <https://doi.org/10.1111/geb.13180>.

Gough, Christopher M., Foster, Jane R., Bond-Lamberty, Ben, Tallant, Jason M., 2022. Inferring the effects of partial defoliation on the carbon cycle from forest structure: challenges and opportunities. *Environ. Res. Lett.* 17 (1). <https://doi.org/10.1088/1748-9326/ac46e9>.

Greinwald, Konrad, Dieckmann, Lea Adina, Schipplick, Carlotta, Hartmann, Anne, Scherer-Lorenzen, Michael, Gebauer, Tobias, 2021. Vertical root distribution and biomass allocation along proglacial chronosequences in central Switzerland. *Arct. Antarct. Alp. Res.* 53 (1). <https://doi.org/10.1080/15230430.2020.1859720>.

Hardiman, Brady S., Bohrer, Gil, Gough, Christopher M., Vogel, Christopher S., Curtis, Peter S., 2011. The role of canopy structural complexity in wood net primary production of a maturing northern deciduous forest. *Ecology* 92 (9). <https://doi.org/10.1890/10-2192.1>.

Hardiman, Brady S., Gough, Christopher M., Butnor, John R., Bohrer, Gil, Detto, Matteo, Curtis, Peter S., 2017. Coupling fine-scale root and canopy structure using ground-based remote sensing. *Remote Sens.* 9 (2). <https://doi.org/10.3390/rs9020182>.

Hardwick, Stephen R., Toumi, Ralf, Pfeifer, Marion, Turner, Edgar C., Nilus, Reuben, Ewers, Robert M., 2015. The relationship between leaf area index and microclimate in tropical forest and oil palm plantation: forest disturbance drives changes in microclimate. *Agric. For. Meteorol.* 201 (February), 187–195. <https://doi.org/10.1016/J.AGRFORMAT.2014.11.010>.

He, Lingli, Ivanov, Valeriy Y., Bohrer, Gil, Thomsen, Julia E., Vogel, Christopher S., Moghaddam, Mahta, 2013. Temporal dynamics of soil moisture in a northern temperate mixed successional forest after a prescribed intermediate disturbance. *Agric. For. Meteorol.* 180 (October), 22–33. <https://doi.org/10.1016/J.AGRFORMAT.2013.04.014>.

Hickey, Laura J., Atkins, Jeff, Fahey, Robert T., Kreider, Mark T., Wales, Shea B., Gough, Christopher M., 2019. Contrasting development of canopy structure and primary production in planted and naturally regenerated red pine forests. *Forests* 10 (7), 566. <https://doi.org/10.3390/F10070566> 2019, Vol. 10, Page 566.

Hofmeister, K.L., Nave, L.E., Riha, S.J., Schneider, R.L., Walter, M.T., 2019. A test of two spatial frameworks for representing spatial patterns of wetness in a glacial drift watershed. *Vadose Zone J.* 18 (1), 1–17. <https://doi.org/10.2136/VZJ2018.03.0054>.

Högberg, Peter, Nordgren, Anders, Buchmann, Nina, Taylor, Andrew F.S., Ekblad, Alf, Högberg, Mona N., Nyberg, Gert, Ottosson-Löfvenius, Mikael, Read, David J., 2001. Large-scale forest girdling shows that current photosynthesis drives soil respiration. *Nature* 411 (6839). <https://doi.org/10.1038/35081058>.

Hopkins, Francesca, Gonzalez-Meler, Miquel A., Flower, Charles E., Lynch, Douglas J., Czimczik, Claudia, Tang, Jianwu, Subke, Jens Arne, 2013. Ecosystem-level controls on root-rhizosphere respiration. *New Phytol.* <https://doi.org/10.1111/nph.12271>.

Ishii, H.T., Tanabe, S.I., Hiura, T., 2004. Exploring the relationships among canopy structure, stand productivity, and biodiversity of temperate forest ecosystems. *For. Sci.* 50 (3), 342–355.

Kane R., Van Lutz, James A., Roberts, Susan L., Smith, Douglas F., McGaughey, Robert J., Povak, Nicholas A., Brooks, Matthew L., 2013. Landscape-scale effects of fire severity on mixed-conifer and red fir forest structure in Yosemite National Park. *For. Ecol. Manag.* 287. <https://doi.org/10.1016/j.foreco.2012.08.044>.

Katayama, Ayumi, Kume, Tomonori, Komatsu, Hikaru, Ohashi, Mizue, Nakagawa, Michiko, Yamashita, Megumi, Otsuki, Kyoichi, Suzuki, Masakazu, Kumagai, Tomomi, 2009. Effect of forest structure on the spatial variation in soil respiration in a Bornean tropical rainforest. *Agric. For. Meteorol.* 149 (10). <https://doi.org/10.1016/j.agrformat.2009.05.007>.

Lavigne, M.B., Foster, R.J., Goodine, G., 2004. Seasonal and annual changes in soil respiration in relation to soil temperature, water potential and trenching. *Tree Physiol.* 24 (4), 415–424. <https://doi.org/10.1093/TREEPHY/24.4.415>.

Liebman, Eli, Yang, Julia, Nave, Lucas E., Nadelhoffer, Knute J., Gough, Christopher M., 2017. Research article: soil respiration in upper great lakes old-growth forest ecosystems. *BIOS* 88 (3). <https://doi.org/10.1893/0005-3155-88.3.105>.

Lim, Kevin, Treitz, Paul, Baldwin, Ken, Morrison, Ian, Green, Jim, 2003. Lidar remote sensing of biophysical properties of tolerant northern hardwood forests. *Can. J. Remote. Sens.* 29 (5). <https://doi.org/10.5589/m03-025>.

Litton, Creighton M., Raich, James W., Ryan, Michael G., 2007. Carbon allocation in forest ecosystems. *Glob. Chang. Biol.* <https://doi.org/10.1111/j.1365-2486.2007.01420.x>.

Ma, Yuecun, Piao, Shilong, Sun, Zhenzhong, Lin, Xin, Wang, Tao, Yue, Chao, Yang, Yan, 2014. Stand ages regulate the response of soil respiration to temperature in a Larix principis-rupprechtii plantation. *Agric. For. Meteorol.* 184. <https://doi.org/10.1016/j.agrformat.2013.10.008>.

McCarthy, Dawn R., Brown, Kim J., 2006. Soil respiration responses to topography, canopy cover, and prescribed burning in an oak-hickory forest in Southeastern Ohio. *For. Ecol. Manag.* 237 (1–3). <https://doi.org/10.1016/j.foreco.2006.09.030>.

Murphy, Bailey A., May, Jacob A., Butterworth, Brian J., Andrensen, Christian G., Desai, Ankur R., 2022. Unraveling forest complexity: resource use efficiency, disturbance, and the structure-function relationship. *J. Geophys. Res. Biogeosci.* 127 (6), e2021JG006748. <https://doi.org/10.1029/2021JG006748>.

Nadelhoffer, Knute J., 2000. The potential effects of nitrogen deposition on fine-root production in forest ecosystems. *New Phytol.* <https://doi.org/10.1046/j.1469-8137.2000.00677.x>.

Nave, Lucas E., Gough, Christopher M., Perry, Charles H., Hofmeister, Kathryn L., le Moine, James M., Domke, Grant M., Swanston, Christopher W., Nadelhoffer, Knute J., 2017. Physiographic factors underlie rates of biomass production during succession in great lakes forest landscapes. *For. Ecol. Manag.* 397. <https://doi.org/10.1016/j.foreco.2017.04.040>.

Orchard, Valerie A., Cook, F.J., 1983. Relationship between soil respiration and soil moisture. *Soil Biol. Biochem.* 15 (4), 447–453. [https://doi.org/10.1016/0038-0717\(83\)90010-X](https://doi.org/10.1016/0038-0717(83)90010-X).

Ostertag, Rebecca, 1998. Belowground effects of canopy gaps in a tropical wet forest. *Ecology* 79 (4). [https://doi.org/10.1890/0012-9658\(1998\)079\[1294:BEOCGI\]2.0.CO;2](https://doi.org/10.1890/0012-9658(1998)079[1294:BEOCGI]2.0.CO;2).

Parker, Geoffrey R., Harding, David J., Berger, Michelle L., 2004. A portable LiDAR system for rapid determination of forest canopy structure. *J. Appl. Ecol.* 41 (4). <https://doi.org/10.1111/j.0021-8901.2004.00925.x>.

Pregitzer, Kurt S., Laskowski, Michele J., Burton, Andrew J., Lessard, Veronica C., Zak, Donald R., 1998. Variation in sugar maple root respiration with root diameter and soil depth. *Tree Physiol.* 18 (10). <https://doi.org/10.1093/treephys/18.10.665>.

R Core Team, 2021. R: a language and environment for statistical computing. URL R Foundation for Statistical Computing, Vienna, Austria. <https://www.R-project.org/>.

Raich, J.W., Schlesinger, W.H., 1992. The global carbon dioxide flux in soil respiration and its relationship to vegetation and climate. *Tellus B* 44 (2). <https://doi.org/10.1034/j.1600-0889.1992.t01-1-00001.x>.

Renaud, V., Innes, J.L., Dobbertin, M., Rebetez, M., 2011. Comparison between open-site and below-canopy climatic conditions in Switzerland for different types of forests over 10 years (1998–2007). *Theor. Appl. Climatol.* 105 (1). <https://doi.org/10.1007/s00704-010-0361-0>.

Scheuermann, Cynthia M., Nave, Lucas E., Fahey, Robert T., Nadelhoffer, Knute J., Gough, Christopher M., 2018. Effects of canopy structure and species diversity on primary production in upper great lakes forests. *Oecologia* 188 (2). <https://doi.org/10.1007/s00442-018-4236-x>.

Shi, Baoku, Gao, Weifeng, Cai, Huiying, Jin, Guangze, 2016. Spatial variation of soil respiration is linked to the forest structure and soil parameters in an old-growth mixed broadleaved-Korean pine forest in Northeastern China. *Plant and Soil* 400 (1–2). <https://doi.org/10.1007/s11104-015-2730-z>.

Shiklomanov, Alexey N., Bond-Lamberty, Ben, Atkins, Jeff W., Gough, Christopher M., 2020. Structure and parameter uncertainty in centennial projections of forest community structure and carbon cycling. *Glob. Chang. Biol.* 26 (11), 6080–6096. <https://doi.org/10.1111/gcb.15164>.

Steyerberg, E.W., 2009. Clinical prediction models. *Statistics for Biology and Health*. <https://doi.org/10.1007/978-0-387-77244-8>.

Suchewaboripont, Vilanee, Ando, Masaki, Iimura, Yasuo, Yoshitake, Shinpei, Ohtsuka, Toshiyuki, 2015. The effect of canopy structure on soil respiration in an old-growth beech-oak forest in central Japan. *Ecol. Res.* 30 (5). <https://doi.org/10.1007/s11104-015-1286-y>.

Sun, Lijuan, Ataka, Mioko, Kominami, Yuji, Yoshimura, Kenichi, 2017. Relationship between fine-root exudation and respiration of two *Quercus* species in a Japanese temperate forest. *Tree Physiol.* 37 (8). <https://doi.org/10.1093/treephys/tpx026>.

Tanaka, Katsunori, Hashimoto, Shoji, 2006. Plant canopy effects on soil thermal and hydrological properties and soil respiration. *Ecol. Model.* 196 (1–2). <https://doi.org/10.1016/j.ecolmodel.2006.01.004>.

Taskinen, Olli, Ilvesniemi, Hannu, Kuuluvainen, Timo, Leinonen, Kari, 2003. Response of fine roots to an experimental gap in a boreal *Picea abies* forest. *Plant and Soil* 255 (2). <https://doi.org/10.1023/A:1026077830097>.

Villegas, Juan Camilo, Breshears, David D., Zou, Chris B., Royer, Patrick D., 2010. Seasonally pulsed heterogeneity in microclimate: phenology and cover effects along deciduous grassland-forest continuum. *Vadose Zone J.* 9 (3), 537–547. <https://doi.org/10.2136/VZJ2009.0032>.

Wales, Shea B., Kreider, Mark R., Atkins, Jeff, Hulshof, Catherine M., Fahey, Robert T., Nave, Lucas E., Nadelhoffer, Knute J., Gough, Christopher M., 2020. Stand age, disturbance history and the temporal stability of forest production. *For. Ecol. Manag.* 460. <https://doi.org/10.1016/j.foreco.2020.117865>.

Wang, Chao, Ma, Yinlei, Trogisch, Stefan, Huang, Yuanyuan, Geng, Yan, Scherer-Lorenzen, Michael, He, Jin Sheng, 2017. Soil respiration is driven by fine root biomass along a forest chronosequence in subtropical China. *J. Plant Ecol.* 10 (1), 36–46. <https://doi.org/10.1093/jpe/rtw044>.

Xiao, Jingfeng, Chevallier, Frederic, Gomez, Cecile, Guanter, Luis, Hicke, Jeffrey A., Huete, Alfredo R., Ichii, Kazuhito, et al., 2019. Remote sensing of the terrestrial carbon cycle: a review of advances over 50 years. *Remote Sens. Environ.* 233. <https://doi.org/10.1016/j.rse.2019.111383>.

Zhou, Zhengchao, Shangguan, Zhouping, 2007. Vertical distribution of fine roots in relation to soil factors in *Pinus tabulaeformis* Carr. forest of the Loess Plateau of China. *Plant and Soil* 291 (1–2). <https://doi.org/10.1007/s11104-006-9179-z>.